The Role of Microtubule Dynamics in Growth Cone Motility and Axonal Growth

Elly Tanaka, Tran Ho, and Marc W. Kirschner

Department of Biochemistry, University of California, San Francisco, California 94143-0448

Abstract. The growth cone contains dynamic and relatively stable microtubule populations, whose function in motility and axonal growth is uncharacterized. We have used vinblastine at low doses to inhibit microtubule dynamics without appreciable depolymerization to probe the role of these dynamics in growth cone behavior. At doses of vinblastine that interfere only with dynamics, the forward and persistent movement of the growth cone is inhibited and the growth cone wanders without appreciable forward translocation; it quickly resumes forward growth after the vinblastine is washed out. Direct visualization of fluorescently tagged microtubules in these neurons shows that in the absence of dynamic microtubules, the remaining mass of polymer does not invade the peripheral lamella and does not undergo the usual cycle of bundling and splaying and the growth cone stops forward movement. These experiments argue for a role for dynamic microtubules in allowing microtubule rearrangements in the growth cone. These rearrangements seem to be necessary for microtubule bundling, the subsequent coalescence of the cortex around the bundle to form new axon, and forward translocation of the growth cone.

THE development of the nervous system proceeds by the extension of long processes from neuronal cell bodies, which travel along complex paths to reach target cells (37). It is known that soluble chemotactic factors, components of the extracellular matrix, and proteins closely associated with the cell surface provide information or at least act as permissive factors for the growth of the axons and dendrites (17, 26, 29, 31, 36, 45). It is thought that the growth cone, the motile portion of the axon terminal, responds to these cues and uses these signals to control the assembly of the neurite process (7, 23, 48). How the growth cone interprets these signals and translates these extracellular cues into the changing morphology of the growth cone is largely unknown. In addition, since the process of axon elongation requires new cellular components, which the axon does not provide, synthesis and the assembly must be coordinated with growth cone motility.

Vesicular materials and secreted proteins are transported along microtubules in the axon, but the structural components of the cytoskeleton do not appear to be transported by the same processes (13, 14, 33, 34). Therefore, an important unanswered question is how these structural components of the axon are transported and assembled. This appears to be closely connected to the problem of morphogenesis of the neuron. The spatial organization of the axon, its morphology and orientation, depend on the cytoskeleton, so ultimately the extracellular guidance cues must be translated into the assembly and arrangement of the cytoskeletal elements. In recent years both the actin and microtubule cytoskeleton system of neurons have been investigated. The dynamic properties of actin in the growth cone appear to be similar to the dynamic properties of actin in motile cells, such as fibroblasts, although the mechanism of transport of actin to the growth cone remains a mystery (19, 35). Microtubules, though well studied as substrates for vesicular transport, have a less obvious role in growth cone morphogenesis. Microtubules form dense bundles in the axon and these bundles extend into the growth cone where they splay out into dynamic single microtubules (8, 10, 50). While it is clear from pharmacological studies that microtubules are necessary for axon growth and stability, their precise role in growth cone motility is unclear (15, 16, 49).

Recent observations of the distribution and behavior of growth cone microtubules, particularly those that visualize the changing microtubule distributions in living cells, suggest that they may be important in guiding directed movement of the growth cone. First, ultrastructural and immunohistochemical studies show that microtubules extend deep into the actin-rich lamella, often to the base of filopodia (9, 21, 27). Second, observations of microtubules in living growth cones showed that in some cases microtubule behavior predicted growth cone behavior. For example, in frog neurons that undergo spontaneous turns in culture, the asym-

Address all correspondence to Elly Tanaka, Ludwig Institute for Cancer Research, Middlesex Hospital/ University College Branch, 91 Riding House Street, London W1P 8BT, England.

© The Rockefeller University Press, 0021-9525/95/01/139/17 $2.00

metric placement of microtubules in the growth cone appears to precede the development of a similar asymmetry in the growth cone, which in turn predicts the spontaneous turn (44). Grasshopper pioneer neurons explanted in the developing limb, initiate stereotypic turns when a filopodium of the growth cone encounters specific guidepost cells. Immediately after that encounter, microtubules invade that branch arising from that specific filopodia, a process that causes that branch to develop into a new axon (39). In encounters between *Aplysia* growth cones, turning is preceded by both changes in the local actin and microtubule distributions (30).

At a higher level of resolution, the process of axon elongation and axon turning can be broken down into three subprocesses: microtubule dynamics, forward and lateral translocation, and bundling of microtubules. Microtubule bundling clearly appears to be an important step in axon formation, preceding the collapse of the lateral membranes around the bundle and the rapid extension of a distal lamellipodium. It is much less clear whether the exploration of peripheral lamellae by dynamic microtubules or forward translocation of masses of microtubules are important in directing growth cone movement (44).

To test the role of dynamic microtubules in growth cone motility and axon elongation, we have used low doses of vinblastine to inhibit microtubule dynamics. Although high concentrations of antimicrotubule drugs cause disassembly of existing microtubules and induce growth cone collapse, recent studies show that low doses of vinblastine can have subtle effects on suppressing dynamics in vitro and in turn affecting processes like mitosis without perturbing the total polymer mass in vivo (3, 24, 25, 46, 51). We hoped that low doses of vinblastine would allow us to suppress microtubule dynamics in the growth cone of frog neurons without affecting the integrity of the existing axonal microtubule array. Using rhodamine tubulin and digital and video microscopy, we have correlated growth cone motility with microtubule behavior during vinblastine treatment. These experiments show that inhibiting the dynamic exploration of growth cone lamellae by microtubules does not perturb overall growth cone motility, but abolishes directional growth cone movement and axon elongation. The microtubules are locked in a nondynamic array that does not proceed through the subsequent steps of microtubule bundling, a step that may be essential for normal axonogenesis. These observations suggest that microtubule dynamics play a necessary role in both axon extension and in spatially constraining of growth cone motility. We speculate that dynamic microtubules play a special role in controlling the orientation of more stable microtubules. Orientation of the microtubule array is likely to be a key step growth cone turning.

Materials and Methods

Xenopus Neural Tube Cultures

Neurons from neural tube explants were cultured as described previously (44). Briefly, dorsal regions were dissected from stage 22–24 *Xenopus* embryos and placed in 1 mg/ml collagenase in Steinberg's solution. After 40 min, neural tubes were further dissected and stored in Steinberg's media until further use (15–30 min). Neural tubes were plated as explants on large coverslips (35 × 50 mm; Carolina Biological Supply, Burlington, NC) coated with Matrigel as previously described.

Fibroblast cells were cultured from dorsal tissue of stage 24 embryos. Instead of using embryo extract, media was supplemented with the defined media supplement, 5% Ultroser HY. This promoted spreading of non-neuronal cells. All other manipulations of the cells are as described for neurons.

Perfusion Chamber

Perfusion chambers were constructed on large rectangular coverslips (35 × 50 mm) that had been acid-cleaned with 1 N HCl for 12 h at 65°C. 22 × 22 mm, 1.5 thickness coverslips were cut into 3 × 22-mm strips, coated on both sides with high vacuum grease, and attached to the large coverslip parallel to each other 15 mm apart so that they made 15 × 22 rectangular flow cell between them. The area between the strips was coated with Matrigel and washed as previously described. The area was then flooded with Steinberg's plating media containing 0.3% methylcellulose (Dow Corning, Barry, U.K.), and the coverslips were placed in a humidified chamber. Neural tube explants were then plated between the strips and allowed to attach and send out neurites for 8–16 h, depending on the type of experiment. Just before observation, the perfusion chamber was sealed by placing a 22 × 22-mm coverslip on top, making sure that plating media filled the volume between the coverglasses.

Time-Lapse Observation of Vinblastine Treatment

For phase observations, cells in the perfusion chamber were observed on a microscope (IM35; Carl Zeiss, Inc., Thornwood, NY) at magnifications ranging from 25 to 60× and recorded using a video rate CCD camera (Hamamatsu Photonic Sys. Corp., Bridgewater, NJ) to an optical memory disk recorder (model 2025; Panasonic Corp., Secaucus, NJ) via an image processing system (Image-1; Universal Imaging, West Chester, PA). All growth rate measurements were made using Image-1.

For perfusion of control, vinblastine, or wash media through the chamber, 150 μl Steinberg's/0.3% methylcellulose with or without vinblastine was added to one side of the chamber and wicked through by placing wedges of paper (No. 1; Whatman Laboratory Products Inc., Clifton, NJ) on the other side. This was repeated three times. Vinblastine was stored as 10 μg/ml stock in H_2O at −20°C, and diluted before each experiment.

For observation of microtubules during vinblastine treatment, *Xenopus* eggs were injected with rhodamine-labeled tubulin as previously described (44). For observation, explants were plated in perfusion chambers as for phase observations. To maintain anoxic conditions, the coverslip was attached to a custom built chamber that covered the perfusion chamber, but had inlets for nitrogen input, two hypodermic needle inputs for adding media for washes, and a thin slit for inserting the wicking paper. The constant flow of nitrogen through the chamber maintained an anoxic atmosphere. The vinblastine and wash media for perfusion were made anoxic by incubation in a nitrogen-filled glove box for 15–20 min with occasional shaking. After incubation, the media was sucked into 1-ml syringes and sealed by inserting it into a hypodermic needle plunged into a rubber stopper. The syringes were then transferred to the cell chamber that had been perfused with nitrogen. Before observation, the cells were perfused with wash media from the syringe both as a control and to ensure that they were growing in anoxic conditions.

Fluorescence Localization of Actin and Microtubules in Growth Cones

Neural tubes explants were grown in the perfusion chambers as described above, but without nitrogen flow. Cells were treated with 10 nM vinblastine in media for 50 min and washed. The samples were fixed at various times during the treatments by flowing in cytoskeletal buffer (43): 10 mM MES, pH 6.0, 138 mM KCl, 3 mM $MgCl_2$, and 2 mM EGTA with 0.5% glutaraldehyde for 10 min. Cells were then extracted with the same buffer with 0.05% Triton X-100 and without fixative for 10 min. Extraction buffer was then replaced with 0.1% sodium borohydride in PBS for 7 min. After washing with PBS, cells were stained with 1 μg/ml rhodamine-phalloidin (Sigma Immunochemicals, St. Louis, MO) for 20 min, then washed with 2% BSA in PBS, then stained with a mouse monoclonal antibody against α-tubulin (DM1α, 1:2,000), washed with PBS, then followed by a fluorescein-labeled donkey anti-mouse antibody (Jackson ImmunoResearch Laboratories, Inc., West Grove, PA). After washing with PBS, chamber was perfused with 80% glycerol, 10 mM Tris, pH 7.8, with 20 mM propylgallate. Samples were stored at −20°C.

Fluorescence Imaging

Microtubules were imaged on a microscope (IMT-2; Olympus Corp., Lake

Success, NY) with a 60×/1.4NA objective. Mercury light was attenuated to 7–12% of full illumination with neutral density filters, and light was shuttered to 0.1-s exposures. Images were acquired onto a cooled CCD camera with a 1024AB chip (Tektronix, Inc., Beaverton, OR). The field was magnified ~270-fold to the chip so that 0.107 μm was imaged onto one pixel width. Images were acquired and processed using a Sun Sparcstation +1, running software from Inovision Corp. (Research Triangle, NC). For viewing of sequences and crude analysis, digital images were transferred to optical disk. All fluorescence intensity measurements were made directly from digital images using the ISee software from Inovision.

For analysis of microtubule growth and shrinkage rates, the growth and shrinkage histories for individual microtubules were generated by measuring the length of the microtubule (from a fixed point on the microtubule) in each successive frame. Growth and shrinkage rates were calculated from the slopes of an entire growth or shrinkage phase. Microtubules that moved laterally were not measured.

Results

Low Doses of Vinblastine Induce Growth Cone Wandering

We initially tested whether application of vinblastine below the concentration that caused distortion and collapse of the growth cone had measurable effects on growth cone motility and axon elongation. Growing frog neurons explanted onto Matrigel from the neural tube of postneurula stage embryos (stage 22) were observed using phase optics by time-lapse video microscopy. They were first perfused with normal media (control) to establish the baseline reaction of the cells to perfusion. After 10–30 min, they were perfused with vinblastine-containing media and then observed for 25–60 min. The vinblastine was subsequently washed out, and the cells were observed for another 30–60 min.

Before vinblastine treatment, the net motion of the growth cone, along the direction of the axon was usually straight, although lamellae transiently extended from the growth cone in all directions. We referred to the net movement of the growth cone along this vector as the forward movement of the growth cone. Perfusion of control media did not affect this vectorial movement. Fig. 1, *0–10 min*, shows a typical growth cone before vinblastine treatment. At 0 min, the growth cone had extended a lamella at ~30° away from the vector of forward movement of the axon (*arrowhead*). By 5 min, the growth cone, which had continued to move in the direction of the axon, had transiently extended lamellae and branches in three directions (*arrowheads*). By 10 min, it had moved forward in roughly a straight line to 40 μm from its position at 0 min.

Examination of 13 explanted neurons showed that in 5–20 nM vinblastine, the growth cone maintained its motile properties, continuing to extend and retract lamellae and filopodia. Tracking of the growth cone showed, however, that it no longer maintained persistent, directed movement, and the rate of axon formation decreased. Rather, the entire growth cone would explore the area around it, often extending a lamella or branch laterally then moving in the direction of that lamella, then exploring another branch or lamella, a behavior that we termed "wandering." Fig. 1, *14–37 min*, shows a typical reaction of a growth cone to vinblastine. Immediately after vinblastine perfusion, the growth cone looks relatively normal (Fig. 1, *14 min*). By 20 min, the growth cone had ceased forward movement, and by 25 min, it had begun moving laterally toward the upper right corner of the field. 6 min later, however, a lateral sprout at the base of the growth cone (*asterisk*), forms a thin veil, which thickens, and pulls on the growth cone (*37 min*). In many cases, this behavior resulted in the formation of branched configurations, as shown in Fig. 1, *37 min*. Under these conditions, the net elongation rate of the axon decreased markedly, while the area of exploration increased.

The effect of vinblastine was easily reversible, and upon washout, the growth cones resumed more persistent forward movement resuming normal rates of axonal elongation. In Fig. 1, by 74 min, when the vinblastine has been washed out, the lower branch (*asterisk*) became the dominant one, and a new growth cone sprouted from the end of it (*80 min*). This growth cone then resumed forward movement so that by 91 min, the axon had extended 38 μm. Note that after vinblastine washout, the growth cone started moving persistently in a direction different from its original course before vinblastine treatment. The axon had apparently lost any influence on the new direction of growth cone movement. Of 13 growth cones treated with 5–20 nM vinblastine, 10 began wandering. Of the remaining growth cones, one rounded up and essentially stopped, and two continued to grow fairly normally. We believe the heterogeneity of response, such as the two growth cones growing normally, is caused by the natural heterogeneity in the cultures, since in one case where we saw a growth cone continue to grow normally in vinblastine, another growth cone in the same field was wandering.

Vinblastine Affects Directional Growth Cone Movement, but Not Overall Motility. From our visual observations of the time-lapse sequences, it appeared that when treated with vinblastine, growth cones lost their persistent forward movement, but that their motility, their ability to move by extending and retracting filopodia and lamellae, was not affected. To distinguish semiquantitatively between vinblastine's effect on persistent directed movement (or axonal elongation) and growth cone motility, we measured the growth cone behavior by three different methods, illustrated for three growth cones in Fig. 2. In Fig. 2 *A*, the trajectory of the growth cone is plotted by simply tracing the x, y coordinates of the growth cone centroid at 1-min intervals. The arrow shows the direction of time, while the instantaneous velocity of movement can be inferred by the distance between the points. The time of buffer, vinblastine, and wash buffer perfusion are indicated by c, v, and w, respectively. At 5 nM, vinblastine addition (*v*) only slightly affects growth cone movement. Intermittently after vinblastine treatment at 60, 70, and 90 min (Fig. 2 *A*, *asterisk*), the growth cone briefly wanders to the side and steps back before resuming some growth. In contrast, at 10 nM, the effect of vinblastine is apparent after 8 min. At 75 min, the growth cone wanders back along the direction in which it was growing, and then starting at 90 min, stalls in one spot until the vinblastine is washed out (*w*). At 20 nM (Fig. 2 *A*), the effect is drastic. In this case, the growth cone had spontaneously begun to move backwards. With the addition of vinblastine, it remains stalled in a small area throughout vinblastine treatment. The neuron did not recover persistent movement until ~15 min after washing out vinblastine. At 50 and 200 nM vinblastine, growth cones collapsed, and the neurites began to retract (data not shown).

To quantitate the effect of vinblastine treatment on forward motion or axon elongation, we calculated the instantaneous

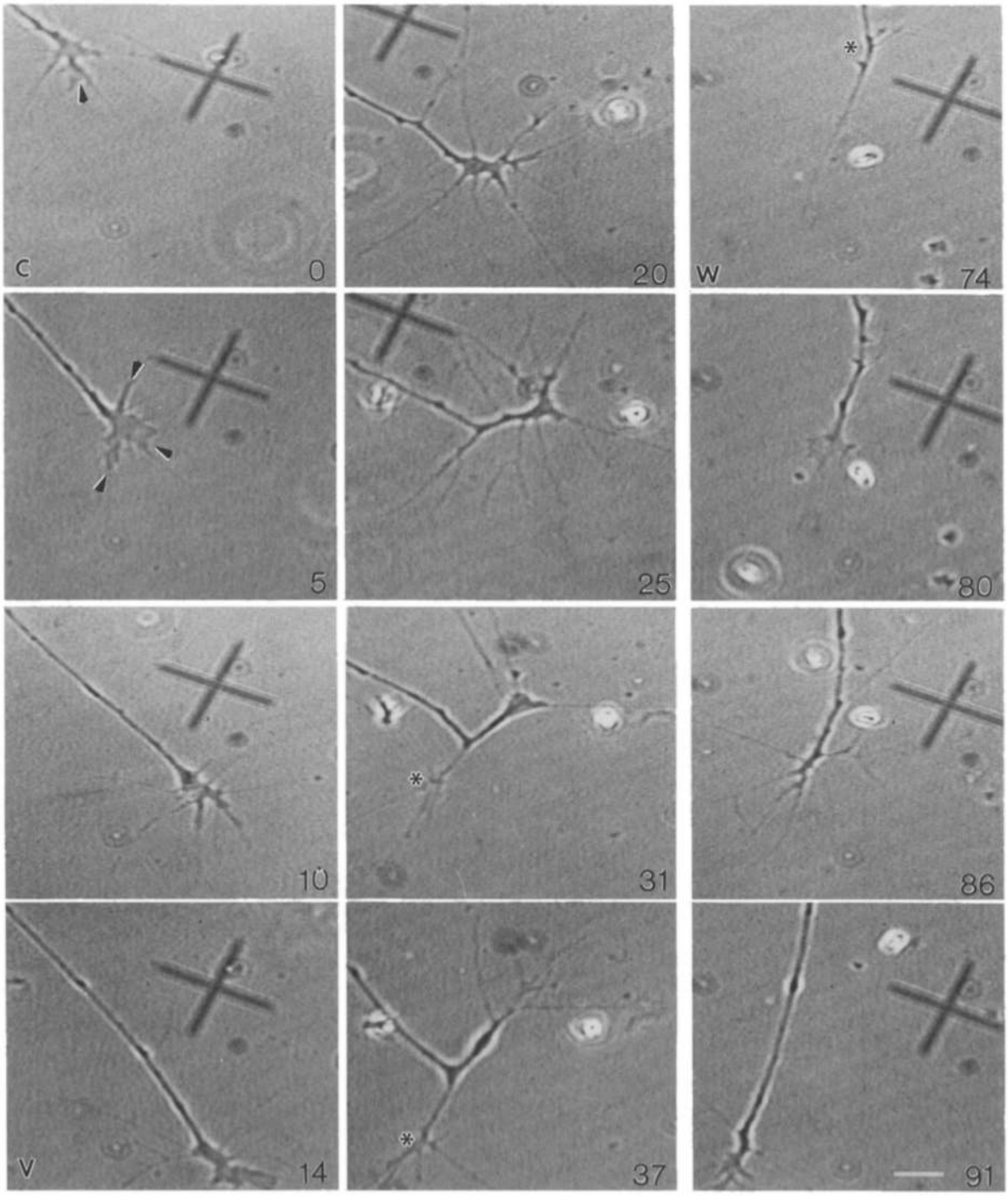

Figure 1. Time-lapse sequence of a growth cone responding to 10 nM vinblastine. Before vinblastine treatment (*c*), the growth cone moves along a straight line, resulting in rapid axonal elongation. In 14 min, the growth cone has traveled 34 μm. Arrowheads at 0 and 5 min show lamellae that are transiently extended in multiple directions, while the growth cone generally proceeds toward the bottom right corner of the field. Vinblastine was added at 11 min (*v*). At 20 min (9 min after vinblastine addition), the growth cone has stopped its forward progression, and by 25 min, has begun exploring laterally. At 37 min, the growth cone is shrinking back from its upper branch, and the lower branch (*asterisk*) is gaining dominance. Vinblastine was washed out at 66 min (*w*). By 74 min, the lower branch (*asterisk*) is remaining, and a growth cone sprouts from its end at 80 min. At 86 min, that growth cone has consolidated into new axon, and the growth cone has continued to move forward at 91 min. The frame of reference is the same for 0–14 min. It is changed but constant for 20–37 min, and then again, for 74–91 min. The white asterisks in frames 37 and 74 mark approximately the same spot on the substrate. Bar, 10 μm.

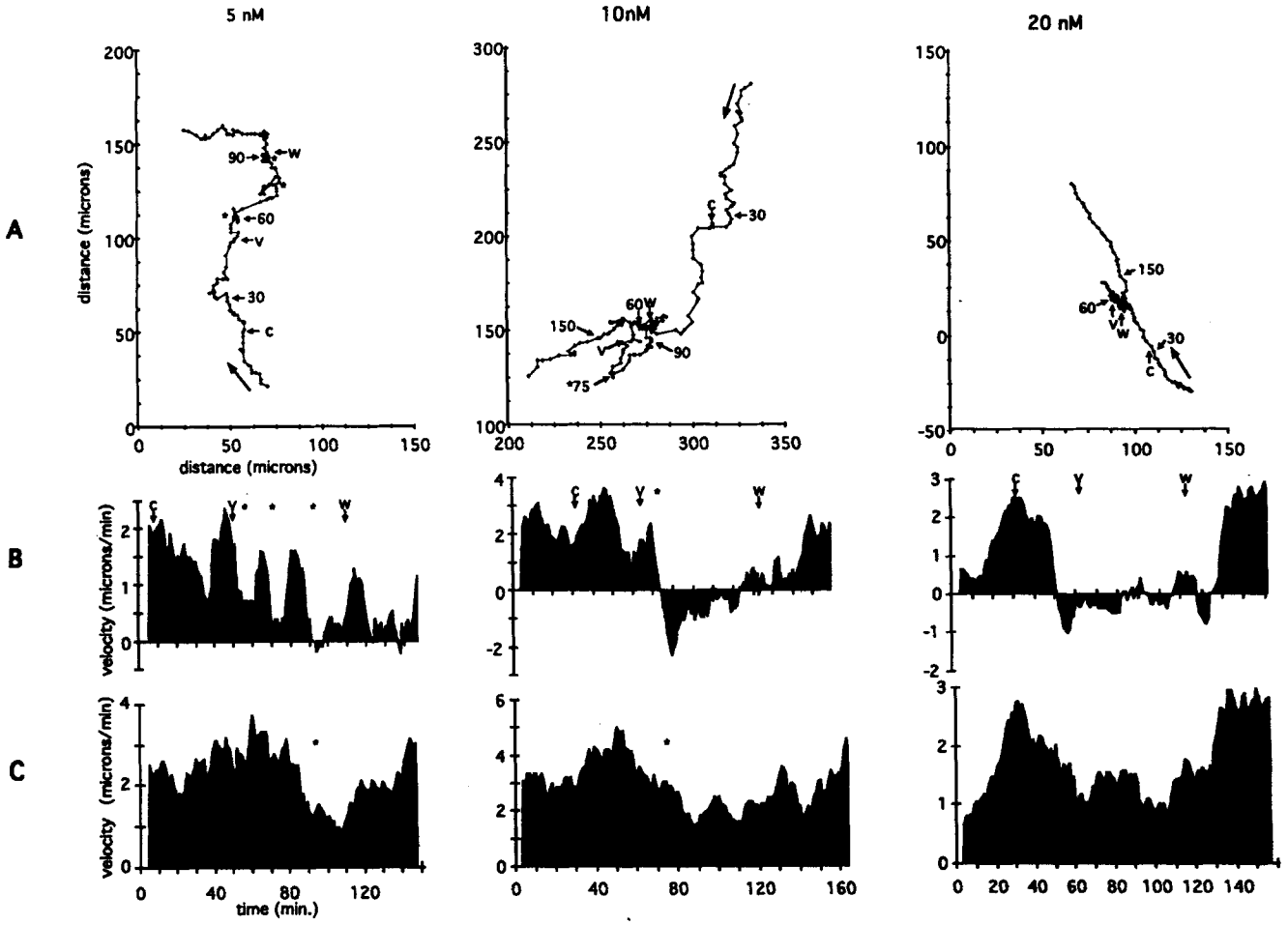

Figure 2. (*A*) Growth cone trajectories of three neurons treated with 5, 10, and 20 nM vinblastine. Each point represents the x, y position of the growth cone centroid at a given time with constant time between each point (1 min). The large arrow at the beginning of each trajectory denotes the direction of growth cone movement and axonal growth. At point (*c*), control media is washed through, (*v*) vinblastine is washed in, and (*w*), vinblastine is washed out. Asterisks denote times during vinblastine incubation where the growth cone wanders astray from a uniform path. (*B*) Growth cone velocity along the direction of growth. The distance of each point from the initial point of each trajectory shown in (*A*) was calculated, and the instantaneous velocity was calculated from these distances. Plot represents the running average of five instantaneous velocities with respect to time. (*C*) Absolute growth cone velocity. Instantaneous velocities were calculated from the distance between each point. Plots represent the running average of five growth cone instantaneous velocities with respect to time.

velocity with respect to the growth cone's starting point, in other words, the rate at which the growth cone was moving away from its starting point. This was done by calculating a vector (v_p) from the initial position of the growth cone of the time-lapse sequence to the centroid of the growth cone for each frame (at 1-min intervals). This results in a series of vectors between the initial point and each point of the trajectory. After taking the magnitude of the vector ($|v_p|$), we subtracted from each vector magnitude, the one from the previous frame ($|v_p| - |v_{p-1}|$). Since the points were 1 min apart, this calculation yielded the instantaneous velocity (truly speed) of the growth cone with respect to the first point of the graph. This analysis is a crude indicator of the persistent movement of the growth cone. If the growth cone retracts or moves backwards, the velocity is negative, if the growth cone slows, the velocity approaches 0, and if the growth cone wanders laterally, the velocity also approaches 0. We will refer to this velocity measurement as persistent velocity. Fig. 2 *B* represents a plot of the running average over 5 min of the persistent velocity with respect to time. At 5 nM, the dip in the graph at ~70 min reflects the lateral motion seen in Fig. 2 *A*, and the negative values at 90 min reflect some brief backwards movement. By contrast, at 10 nM, the growth cone begins stepping backwards 15 min after vinblastine addition, with a much larger magnitude of backward movement, as compared to the effects at 5 nM (2 vs 0.5 μm/min). At 20 nM, the growth cone hovers around 0 during vinblastine treatment. Therefore, at 10 and 20 nM, there is a marked effect on persistent growth cone advance, which is seen clearly as a valley between the mountains of initial and final growth cone movement under control conditions. The average persistent velocities for 13 growth cones is given in Table I.

As a measure of the general motility properties of the growth cone, i.e., the instantaneous extension of the growth cone without any reference to the initial vector of movement, we measured the absolute velocity of the growth cone by simply calculating the distance, irrespective of direction, between each successive x, y position of the growth cone. Therefore, if the growth cone froze in its tracks, the velocity

Table I. Motility and Persistent Velocities of Neurons Treated with Vinblastine

Concentration	n	Motility velocity				Persistent velocity			
		Precontrol	Control	Vinblastine	Wash	Precontrol	Control	Vinblastine	Wash
		μm/min				μm/min			
5 nM	3								
		2.81	2.09	1.82	2.88	2.35	1.32	0.45	0.98
		6.94	4.69	3.76	3.89	5.64	3.35	1.89	2.06
		2.41	2.56	2.00	2.22	2.04	1.41	0.63	0.56
Average, SD		4.05 ± 2.51	3.11 ± 1.39	2.53 ± 1.07	2.99 ± 0.84	3.34 ± 1.99	2.03 ± 1.15	0.99 ± 0.78	1.2 ± 0.77
10 nM	5								
		3.65	3.93	3.20	4.33	2.92	3.61	−0.03	3.10
		3.07	4.09	2.13	2.89	2.20	2.32	−0.27	1.60
		2.69	2.92	2.66	2.72	0.66	0.91	0.03	1.03
		2.44	1.38	1.46	2.07	1.31	1.14	1.16	1.76
		2.21	3.03	2.09	1.50	1.86	2.86	1.67	1.08
Average, SD		2.81 ± 0.57	3.07 ± 1.08	2.31 ± 0.65	2.70 ± 1.06	1.79 ± 0.86	2.17 ± 1.14	0.51 ± 0.85	1.71 ± 0.84
20 nM	5								
		2.27	2.55	1.72	2.08	1.91	2.12	1.09	1.65
		1.46	1.85	1.23	2.28	1.14	0.91	−0.16	1.74
		3.26	2.80	2.37	2.37	2.95	2.59	0.80	0.80
		3.18	3.60	2.41	2.04	2.86	3.42	−0.72	0.89
		3.20	3.40	2.57	1.98	2.86	2.97	0.86	1.26
Average, SD		2.68 ± 0.79	2.84 ± 0.7	2.06 ± 0.57	2.15 ± 0.17	1.91 ± 0.95	2.04 ± 1.18	0.37 ± 0.77	1.27 ± 0.43

would approach 0, whereas if the growth cone wandered, the motility would remain high. We will refer to this velocity as motility velocity. As seen in Fig. 2 *C*, while it is clear that the motility velocity decreases somewhat upon vinblastine addition, it is reduced far less than the relative velocity. The average decrease of motility for all growth cones in 10 nM is only 25% in contrast to the average decrease of 75% for persistent velocity (Table I). This indicates that the growth cone maintains much, although not all, of its motility during vinblastine treatment. The decrease in persistent velocity without a matching decrease in motility velocity reflects that the growth cone is either exploring a larger lateral area or continues to change shape.

Vinblastine Inhibits Microtubule Dynamics in Nonneuronal Cells

Numerous experiments have shown that vinblastine is a specific inhibitor of microtubule assembly. Whereas high concentrations induce microtubule depolymerization and aggregation into paracrystalline arrays, low concentrations of vinblastine have been shown in vitro to depress microtubule dynamics without changing the relative polymer mass (24, 25). To examine the effects of low concentrations of vinblastine on microtubule dynamics in vivo, the morphology of the nerve cell is disadvantageous because the rapid incorporation of the microtubules into bundles makes it very difficult to follow any one microtubule for an extended period of time and extensive microtubule translocations make it difficult to distinguish polymerization from movement. Cells of a typical fibroblast morphology are more favorable because the microtubules seem not to be subjected to extensive polymer movement and because microtubules are separated from each other; therefore, the length of individual microtubules can usually be followed for a relatively long distance. We examined the microtubules in nonneuronal cells explanted from the neural tube. These fibroblastoid cells extend large, flat lamellae that are optimal for dynamics measurements.

Using the same procedure for fluorescently labeling *Xenopus* neurons with rhodamine-tubulin (44), we cultured neural tubes and somites, but in this case, included serum factors that would stimulate the spreading of nonneuronal cells. Cells were observed under anoxic conditions every 8.5–15 s using epifluorescence microscopy. We measured more than 40 microtubules in both the control and vinblastine, and 28 microtubules during recovery in three cells.

Before vinblastine treatment, microtubules exhibited normal dynamic instability behavior. They alternately grew and shrank at rates and transition frequencies comparable to those measured previously. This behavior is shown in Fig. 3 for microtubule dynamics between time 0 and 36 s. The larger arrow shows a microtubule that begins shrinking at 19 s, and by 36 s, has shrunk 2.5 μm. The smaller arrowheads highlight another shrinking microtubule. These microtubules coexist with growing microtubules that are highlighted by the thin arrows.

In contrast, microtubules in vinblastine treated cells have long periods of pausing, and they have reduced growth and shrinkage rates, making them relatively undynamic (Figs. 3 and 4). In vinblastine, the average growth and shrinkage rate decreased from 6.4 ± 3.25 to 3.1 ± 3.4 μm/min and from 14.3 ± 8.5 to 5.1 ± 4.0 μm/min (mean ± SD), respectively, and the microtubules spent 81% of the time in the paused state as compared to 43% under control conditions. The percentage of time spent growing decreased from 37 to 8%, while time spent shrinking from 21 to 11%. As seen in Fig. 3, the microtubules in vinblastine treated cells undergo very little growth or shrinkage during the time of observation. For example, three microtubules in the periphery (*arrowheads, 56 s–8:53 min*), are still visible after 8 min. The upper one, although it appears to shrink 1.2 μm between 2:33 and 3:51

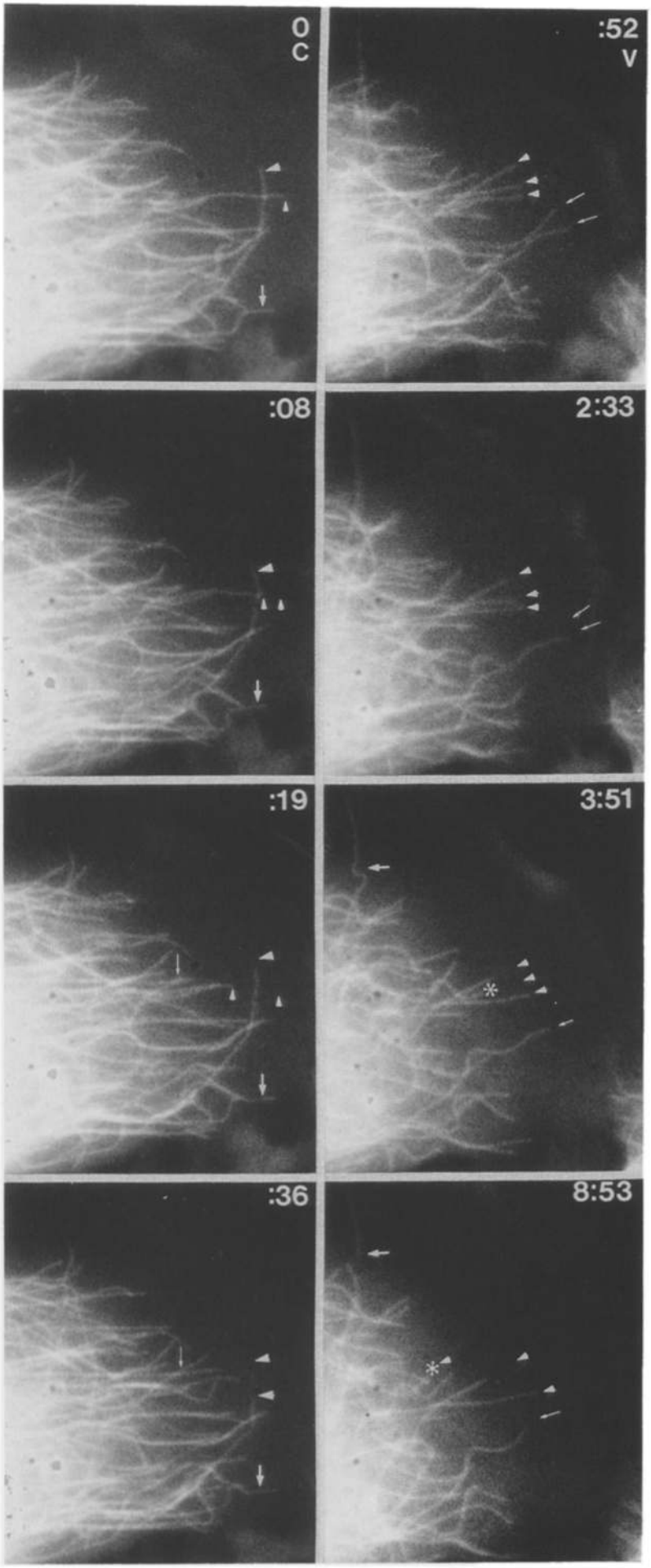

Figure 3. Microtubule dynamics in a nonneuronal cell before, during, and after 10 nM vinblastine treatment. 0–36 s (control [*c*] column) shows microtubule dynamics before vinblastine treatment. Microtubules display typical dynamic instability behavior. Large and small arrowheads highlight two microtubules that undergo rapid shrinkage events, while arrows show microtubules undergoing growth. At 52 s to 8:53 min (vinblastine [*v*] column), the cell has been treated with 10 nM vinblastine. Many microtubules are stable during this interval. Of three microtubules (*arrowheads*), two are stable for the 8-min interval, while one depolymerizes. Similarly, one of the two microtubules (*small arrows*) remains stable while the other depolymerizes. The stable microtubule in the upper left region (*larger arrow*) becomes kinked (*3:51 min*) and is eventually severed (*8:53 min*). Bar, 5 μm.

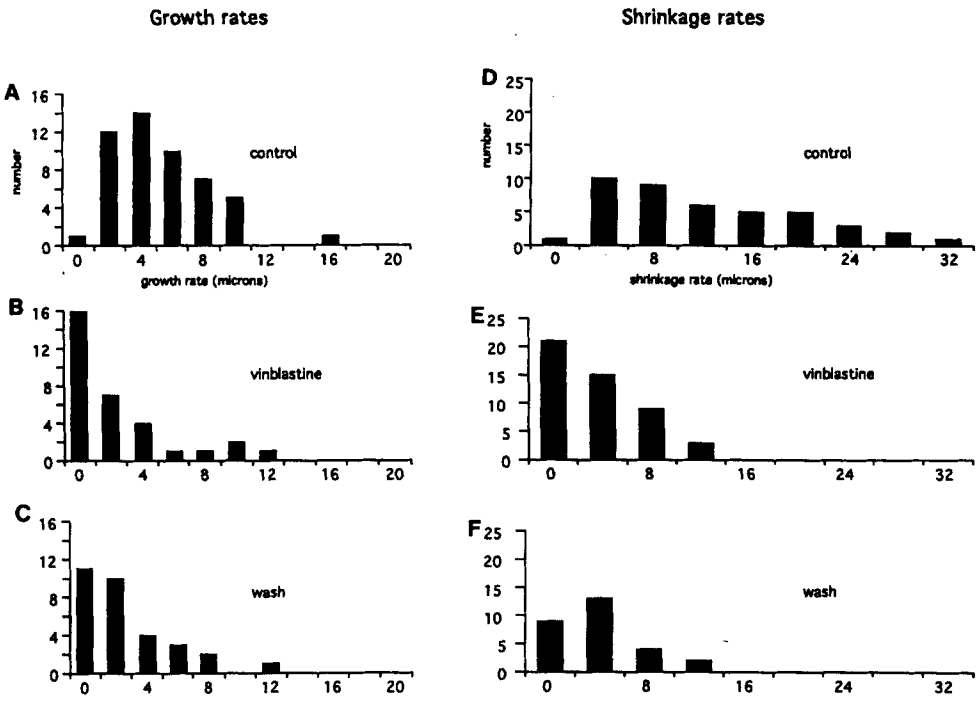

Figure 4. Histograms of growth and shrinkage rates. (*A* and *D*) Growth and shrinkage rates for control cells before vinblastine treatment. Mean growth and shrinkage rates were 6.4 ± 3.25 SD and 14.3 ± 8.5 μm/min, respectively. (*B* and *E*) 10 nM vinblastine-treated cells. Mean growth and shrinkage rates were 3.1 ± 3.4 and 5.1 ± 4.0 μm/min. (*C* and *F*) Cell after washing out vinblastine. Mean growth and shrinkage rates were 3.8 ± 2.8 and 5.6 ± 3.4 μm/min.

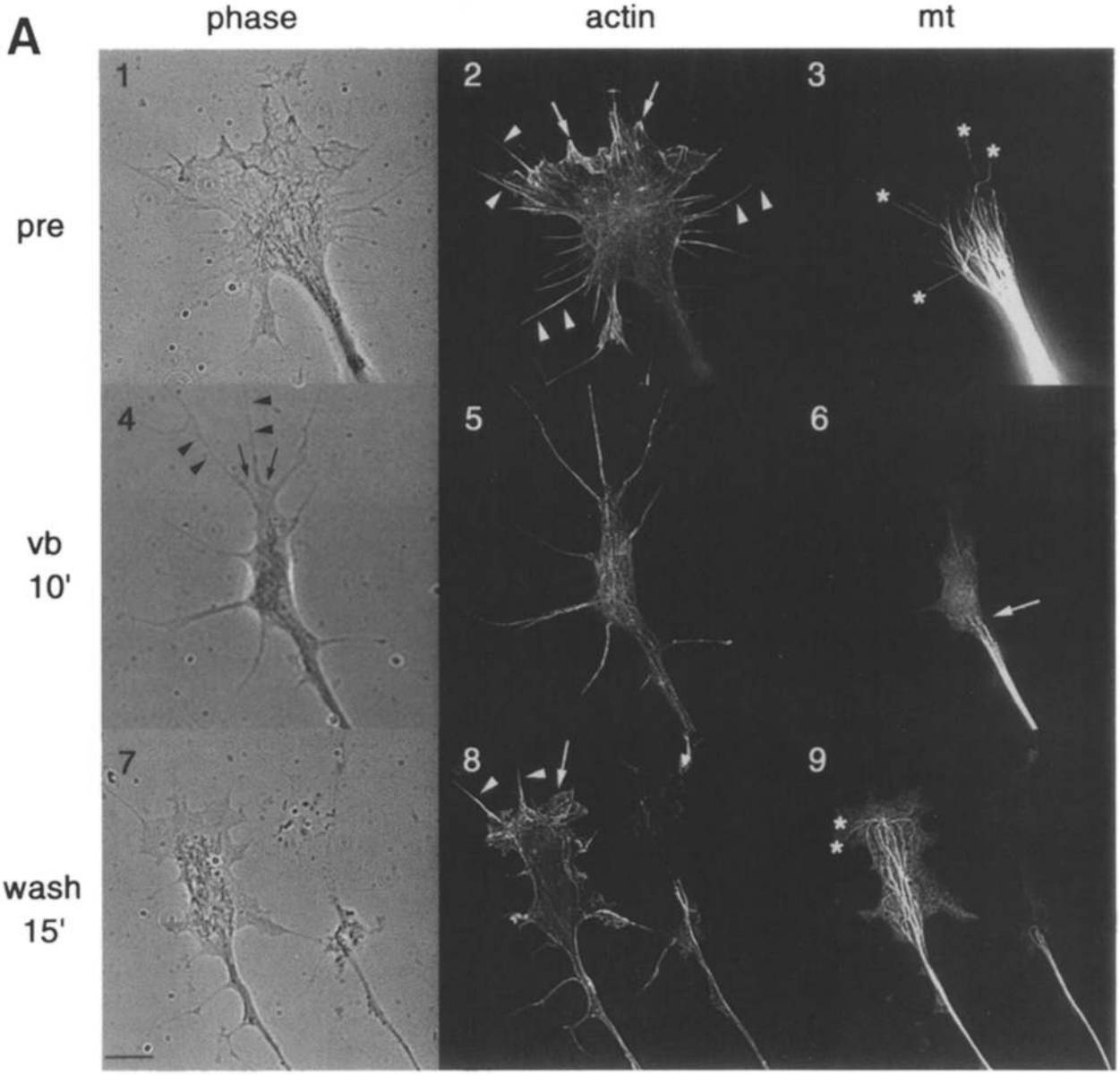

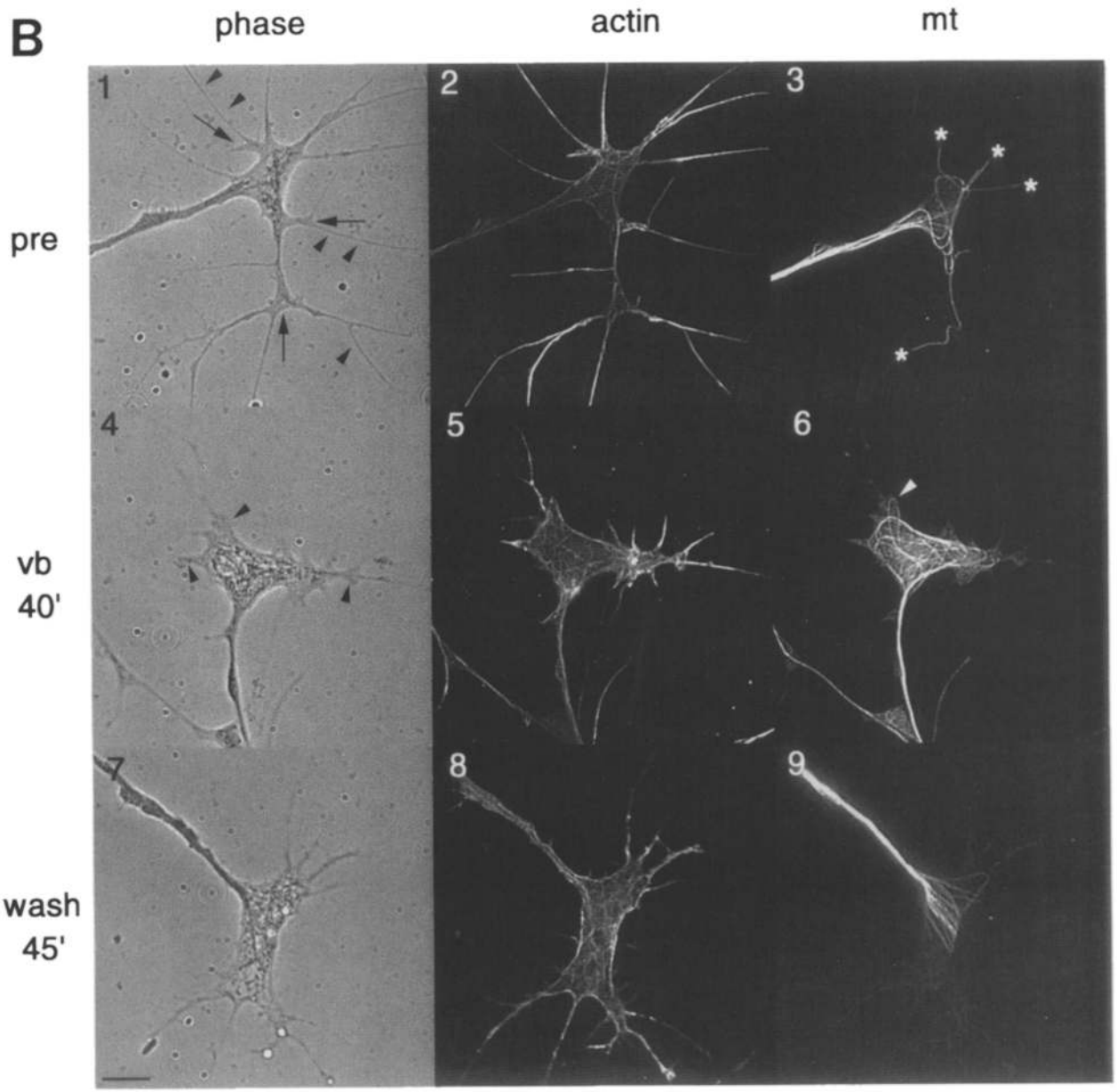

Figure 5. (A_{1-3}) Phase, actin, and microtubule images, respectively, of a growth cone before vinblastine treatment. (A_1) Organelles are limited to the central region of the growth cone leaving large expanses of organelle-free lamella with filopodia extending radially from the growth cone. (A_2) The distal regions of lamellae are actin rich (*arrows*), as are the filopodia, which begin within the growth cone and extend away from it (*arrowheads*). (A_3) Most microtubules terminate in the central region of the growth cone, but some single microtubules (*asterisks*) extend out into the organelle-free regions seen in phase. (A_{4-6}) Phase, actin, and microtubule images, respectively, of a growth cone 10 min after addition of vinblastine. (A_4) The growth cone is spindly, with small veils (*arrows*) spread between filopodia (*arrowheads*). (A_5) While filopodia still contain high concentrations of actin, they do not extend back into the growth cone, and the body of the growth cone contains a uniform meshwork of bundles, without brightly stained structures as seen in the lamellum of (A_1). (A_6) Microtubule bundles only extend to the neck of the growth cone, leaving the growth cone (*arrow*), which still contains organelles, essentially void of microtubules. (A_{7-9}) Phase, actin, and microtubule images, respectively, of a growth cone 15 min after removal of vinblastine. (A_7) The growth cone has flat areas of organelle-free lamella with organelles occupying only the central region. (A_8) The organelle-free areas seen in phase stain brightly for actin (*arrows*), as well as the filopodia (*arrowheads*), while the central region of the growth cone has dimmer, more uniform staining. (A_9) Microtubules primarily occupy the central region of the growth cone and form a looped configuration. Two microtubules extend into the organelle-free periphery (*asterisks*). (B_{1-3}) Phase, actin, and microtubule images, respectively, of a growth cone before vinblastine treatment. In contrast to the growth cone in A_{1-3}, this growth cone has a spindly morphology, where the organelles occupy most of the growth cone, with small veils (*arrows*) extending along and between filopodia (*arrowheads*). (B_2) The actin forms some networks through the body of the growth cone, but is highly concentrated in the filopodia (*arrowheads*). (B_3) The microtubules occupy all regions of the growth cone, forming a contorted mass in the central region, with single microtubules invading deep into the veils and branches (*asterisks*). (B_{4-6}) Phase, actin, and microtubule images, respectively, of a growth cone 40 min after addition of vinblastine. (B_4) The growth cone has remained spread, but organelles occupy the vast majority of the growth cone area. Very small organelle-free areas protrude from various parts of the growth cone (*arrowheads*). (B_5) The large growth cone is criss-crossed crossed with actin cables in the central region of the growth cones, while filopodia protrude from the growth cone. (B_6) In contrast to the growth cone in A_6, microtubules form a highly looped network that fills the entire growth cone. One bent microtubule occupies an organelle free area (*asterisk*). (B_{7-9}) Phase, actin, and microtubule images, respectively, of a growth cone 45 min after removal of vinblastine. (B_7) The growth cone has a spread morphology, but organelles still occupy the major part of the growth cone. (B_8) The actin concentration is high at the edges of the growth cone, and it forms a lightly stained meshwork internally. (B_9) As the microtubules emerge from the neck, they spread to form a splayed configuration. However, in this case, they do not spread throughout the growth cone. Bars, 10 μm.

min, has actually translocated back as the proximal portion of the microtubule towards the cell center becomes kinked. Such microtubules were not included in the measurements. The middle microtubule becomes kinked between 2:33 and 3:51 min, and then eventually shrinks back to the asterisk in 8:53 min. Another microtubule in the upper left (*large arrow*), which is stable throughout the 8 min, also becomes kinked between 2:33 and 3:51 min, and is then actually severed between 3:51 and 8:53 min. Similarly, of two microtubules highlighted by the smaller arrows, the lower one is stable and visible for the entire 8 min, while the upper one shrinks back between 52 s and 2:33 min.

After washing vinblastine out, microtubules began to regain some of their dynamic properties. The proportion of time the microtubules spent pausing decreased from 81 to 58%, while the time spent growing increased from 8 to 26% and the time spent shrinking from 11 to 16%. During the time of observation, the growth and shrinkage rates, however, remained depressed at 3.8 ± 2.8 and 5.6 ± 3.4, respectively (Fig. 4). During recovery from vinblastine, microtubule fragments presumably generated through severing were propelled forward into the lamella; such events were not included in the measurements.

The Distribution of Microtubules and Actin in Vinblastine-treated Growth Cones

Since vinblastine at very low concentrations had dramatic effects on axon elongation and forward cell movement, we examined the effects of vinblastine on microtubules and actin in growth cones by immunohistochemistry. The growth cones in the population were heterogeneous, both in actin and microtubule distribution. The effect of vinblastine was subtle and the heterogeneity between growth cones persisted after vinblastine treatment. Before vinblastine treatment, growth cones ranged from having lamellae rich in actin microspikes that extended centripetally towards the central region (Fig. 5 A_2, *arrowheads*) with additional less organized actin staining in the peripheral areas of the lamellae (Fig. 5 A_2, *arrows*) to more spindle-shaped configurations dominated by filopodia, with veils spanning between filopodia, where filopodia were actin-rich, and the rest of the growth cone was uniformly stained for actin (Fig. 5 $B_{1,2}$). The microtubules displayed the three types of distributions, splayed, looped, and bundled, as described previously (44). In Fig. 5 A_3, the microtubules were splayed with most confined to the central region of the growth cone, but significant numbers extended beyond the organelle-rich region into the organelle-poor lamella (*asterisks*). In contrast, the growth cone in Fig. 5 $B_{1\text{-}3}$ is quite small, dominated by actin-rich filopodia with small veils spreading between them. Contorted microtubules fill the growth cone and reach deep into the organelle-free veils (Fig. 5 B_3, *asterisks*). After vinblastine addition, the actin distribution within the cell appeared more uniform, with no microspikes running from the filopodia into areas of lamellae (Fig. 5, A_5 and B_5). The microtubule distribution between various growth cones remained heterogeneous, still ranging from splayed to looped to bundled (Table II). The percentage of growth cones with a bundled microtubule configuration increased from 26% before vinblastine to 52% (Table II). Most strikingly, of these growth cones with bundled microtubules, the majority had microtubule bundles extending only to the neck. This is shown in Fig. 5 A_6, where the microtubules only extend to the neck of the growth cone (*arrow*), well behind regions containing organelles. Other growth cones maintain large numbers of microtubules in the growth cone. The growth cone in Fig. 5 B_6 that had been in vinblastine for 40 min is filled with looped microtubules. Both the microtubules and the organelles fill most of the growth cone area, while the actin forms a lightly stained network throughout the growth cone with no distinctive lamellipodial staining.

After washing out the vinblastine, growth cones began to regain a flattened, lamellipodial form. The growth cone in Fig. 5 A_7 has significant regions of organelle-free lamellae that have higher actin staining than the central portion of the growth cone (Fig. 5 A_8). In Fig. 5 A_9, microtubules fill the organelle-rich region with two extending beyond into the lamella, while in Fig. 5 B_9, splayed microtubules occupy only the central region of the growth cone.

From the fixed cells, the effects of vinblastine on growth cone microtubules were much less clear and uniform than what could be observed by visualizing the microtubule dynamics in fibroblasts. Therefore, the relationship between the changes in microtubules and growth cone behavior were difficult to understand. The morphology of the growth cones was variable to start with, making the analysis more difficult. Because of the appearance of growth cones that had microtubule bundles extending only to the neck, it seemed that vinblastine may inhibit accumulation of microtubules in the growth cone. Given this interpretation, the presence of growth cones with looped microtubules was difficult to understand from the static images, and it was unclear if this distribution was generated because a growth cone collapsed back, causing the microtubules at the neck to deform, or if the looped microtubules were generated by the accumulation of polymer in the growth cone.

The Effect of Vinblastine on Microtubules in the Growth Cone

To better understand the relationship between the microtubule distribution and growth cone wandering, we observed neurons labeled with rhodamine-tubulin using epifluorescence at time-lapse intervals ranging from 8.4 to 30 s under conditions where vinblastine or control solutions were perfused through the cell chamber. After 10–30 min of exposure, vinblastine was washed out, and we observed the cells for an additional 20–45 min. Of 23 neurons observed, 12 were analyzed in detail. Among the remaining 11, 7 cells

Table II. Microtubule Distributions during Vinblastine Treatment

	Looped	Splayed	Bundled	Bundles at neck	*n*
Before vinblastine	8	9	5	1	23
Vinblastine (10 nM, 10 min)	5	6	5	7	23
Vinblastine (10 nM, 40 min)	7	3	3	8	21
Washout (15 min)	10	3	5	3	21
Washout (45 min)	6	5	8	1	20

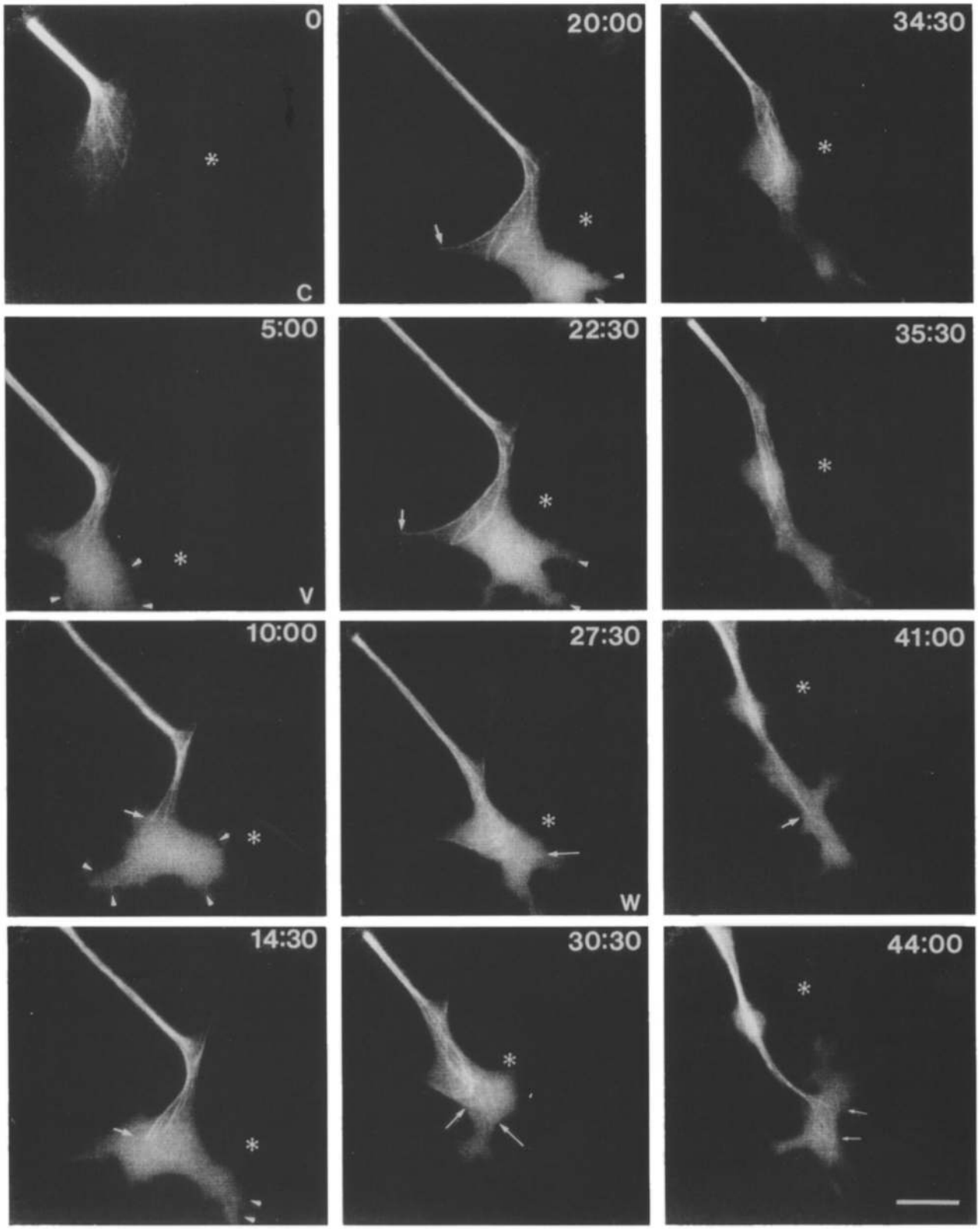

Figure 6. Complete timelapse sequence of microtubules in a growth cone treated with 10 nM vinblastine. Before vinblastine addition (*0 min*), single microtubules spread throughout the growth cone. Just after vinblastine addition (*5 min*), single microtubules can still be seen. During the remainder of vinblastine treatment, sparse bundles of microtubules populate the growth cone. The bundles move forward within the growth cone (*arrows, 10–22:30 min*). During vinblastine treatment, the lamella becomes quite large, but it remains unoccupied by microtubules (*arrowheads, 5–22:30 min*). After vinblastine washout (27:30-44 min), microtubules populate the distal regions of the lamella (*arrows*, 27:30 and 30:30 min). These microtubules become consolidated into a bundle (34:30–41 min), and axon growth resumes. During this rapid outgrowth, a long lamella forms at the end of the growth cone in 35:30 min, but it is quickly invaded by microtubules at 41 and 44 min (*arrows*). The field is moved several times during the sequence; the asterisk marks a constant position on the substrate. Bar, 10 μm.

did not grow significantly after wash out, while 4 cells were too difficult to analyze because they interacted with other cells.

Forward Extension of Microtubules Continues during Vinblastine Treatment. Consistent with our observations in fixed cells, we found that in 5 out of 12 cases, the microtubules in growth cones treated with vinblastine at least transiently assumed a configuration where they only extended up to the neck of the growth cone. To our surprise, however, we found that in 4 out of 12 cases, the microtubule array continued to extend forward slowly and steadily after this distribution was attained. This is illustrated in Fig. 6. In the 15 min before adding vinblastine, the growth cone had moved forward 50 μm. Initially after adding vinblastine, at 5 min, some single microtubules can be seen in the growth cone. At 10 min, only three small bundles remain at the neck of the large growth cone expanse outlined by the arrowheads. These are highly likely to be small bundles because they are brighter than the single microtubules seen at 5 min. Between 10 and 22:30 min, these small bundles extend forward into the growth cone (Fig. 6, *arrow, 10–22:30 min*). The microtubule bundle on the left extends forward at ~0.8 μm/min. Note that between 10 and 22:30 min, the growth cone has not moved forward significantly with respect to the asterisk, which marks a constant point in the field, although the shape of the growth cone has changed and that the microtubules are extending into the growth cone, while there is little forward movement of the growth cone. After washing out the vinblastine at 27:30 min, the microtubules coalesce into a bundle between 30:30 and 41 min. By 41 min, this bundle was associated with significant axon formation (the field was moved to keep the growth cone in view); at 44 min, a new growth cone had formed.

In 3 out of 12 cases, we observed the formation of looped microtubules in vinblastine-treated neurons, which we had previously explained by microtubule translocation (44). In these cases, the distributions were not generated by the growth cone collapsing back onto the microtubules; rather, the growth cone stopped moving forward, and polymer accumulated in the growth cone without forming a coherent bundle. This phenomenon is shown particularly clearly in Fig. 7. At 0 min, the growth cone has just been treated with vinblastine. The microtubules are already somewhat looped, and there is a small bulge containing microtubules in the axon behind the growth cone (*arrow*). At 1:40 min, the microtubules in the neck area (Fig. 7, *arrowheads*) have become contorted by compression caused by microtubule forward translocation into the stalled growth cone. The movement of the microtubule bulge toward the growth cone neck most likely marks the forward translocation of microtubule polymer (Fig. 7, *arrow, 1:40*). At 3 min, the microtubules are even more contorted, and by 6 min, the intensity of fluorescence in the growth cone caused by accumulation of microtubule polymer has become noticeably brighter, while the width and intensity of the axon has diminished. This redistribution of fluorescence is most extreme at 10 min, where the total intensity resulting from microtubules in the growth cone has increased 1.6-fold (arbitrary fluorescence units) from 0 min, while the intensity per unit length in the axon has decreased 2.5-fold. Of the remaining neurons, in two, the microtubules did not continue to extend and the growth cone then collapsed back onto microtubules during vinblastine treatment and subsequently grew back after washing out vinblastine, and in three growth cones, the polymer neither receded back to the neck nor accumulated in the growth cone, but appeared relatively inert. Of these three, two growth cones remained fairly stationary assuming only shape changes, while the other wandered, dragging and deforming the microtubules array, which did not appear to be extending.

Correlation of Microtubule Behavior with Growth Cone Movement. We have described changes in microtubule position and behavior that occur during the treatment of neurons with 10 nM vinblastine. To relate these observations to our initial phase observations of decreased persistent movement, as well as increased growth cone wandering in vinblastine, we followed the growth cone in our fluorescence sequences and correlated the growth cone motility with changes in the microtubule distribution. We analyzed 11 cases in this manner, where the outline of the growth cone could be resolved using the cytoplasmic background produced by the tubulin monomer fluorescence, or from matching phase pictures that were taken alternating with the fluorescence pictures. Vinblastine treatment produced the same effects on growth cone motility as presented earlier and in addition interfered with the usual cycle of microtubule exploration, followed by bundling, followed by forward movement of the growth cone (44). However, as described above, we did not find a specific terminal morphology of the microtubule arrays caused by vinblastine treatment that correlated with the inhibition of growth cone movement.

There was, however, a very good correlation between the reemergence of single microtubules in the lamella and the resumption of persistent growth cone movement when vinblastine was washed out of the culture medium. In 10 of 11 cases, we found that the microtubules reemerged before the resumption of growth. In one case, it was difficult to discern any effect of vinblastine on either the growth cone motility or the microtubule distribution. The lag between microtubule emergence and growth cone movement ranged from 2 to 8 min. Such a relationship can be seen in Fig. 8, which shows a growth cone at the time vinblastine is washed out (0 min). The growth cone did not move significantly between 0 and 4:35 min, yet by the latter time point, three microtubules had already emerged from the distal end of the microtubule bundle. By 17:03 min, when there were many new microtubules, the growth cone had moved ~20 μm (in this last view, the stage had been moved to follow the growth cone; the asterisk marks a constant position on the field).

Discussion

Low Doses of Vinblastine Induce Growth Cone Wandering

We have found that exposure of neurons to 5–20 nM vinblastine had two immediate effects: growth cones lost their persistent forward movement and the rate of axonal elongation was decreased. Under these conditions, the growth cones would "wander," they would explore more lateral areas than during normal growth. The loss of forward movement was not compensated for by an increase in axon length. Both the effect on axonal elongation and growth cone wandering were readily reversible upon removal of vinblastine. These

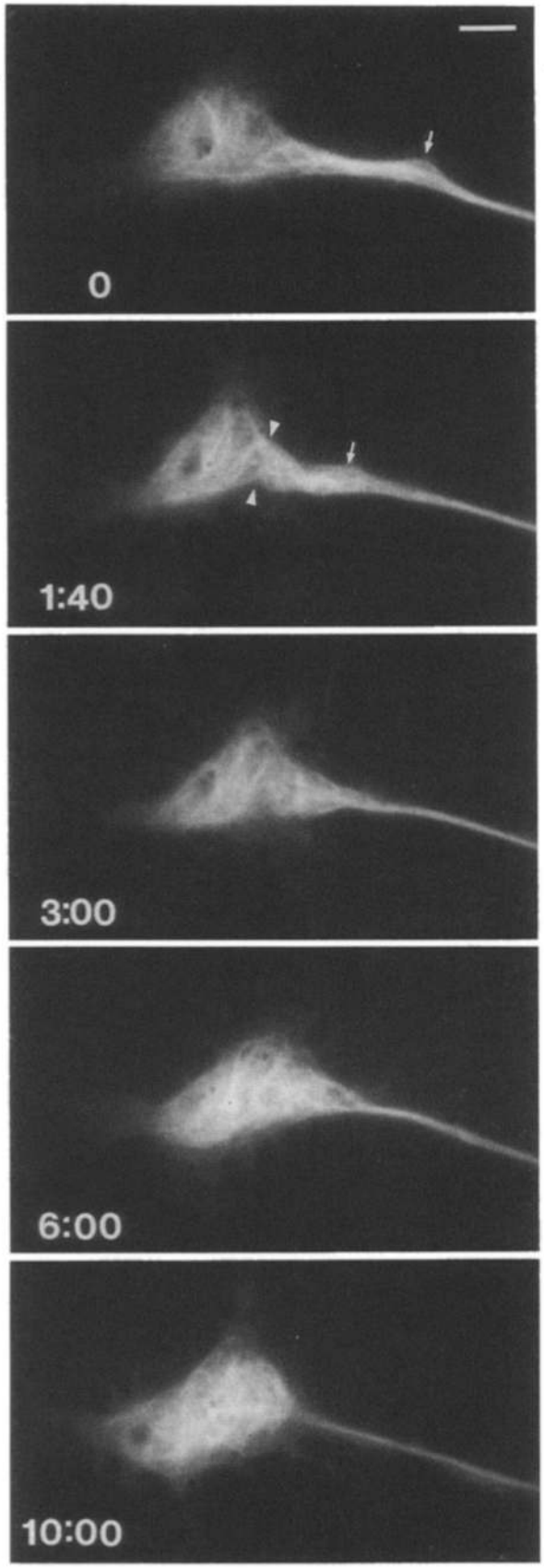

Figure 7. Accumulation of microtubule loops in the growth cone with depletion of microtubules from the axon during vinblastine treatment. The neuron has been treated with vinblastine for 4 min. During the course of 10 min, microtubule loops accumulate in the growth cone by the translocation of microtubules from the axon into a stationary growth cone. The arrow at time 0 and at 1:40 min follows the forward translocation of a nodule of microtubules towards the neck of the growth cone. Comparison of 10 with 0 min shows that the microtubules in the growth cone have become compacted. At the left of the figure is shown the total area and the total intensity of the growth cone microtubules at the various times, while to the right is the intensity per unit length of axonal microtubules. During 10 min, the total intensity of fluorescence signal increased 1.6-fold in the growth cone, reflecting the accumulating polymer, while the fluorescence intensity of the axon per unit length has decreased 2.5-fold, reflecting the depletion of microtubules in the axon. Bar, 5 μm.

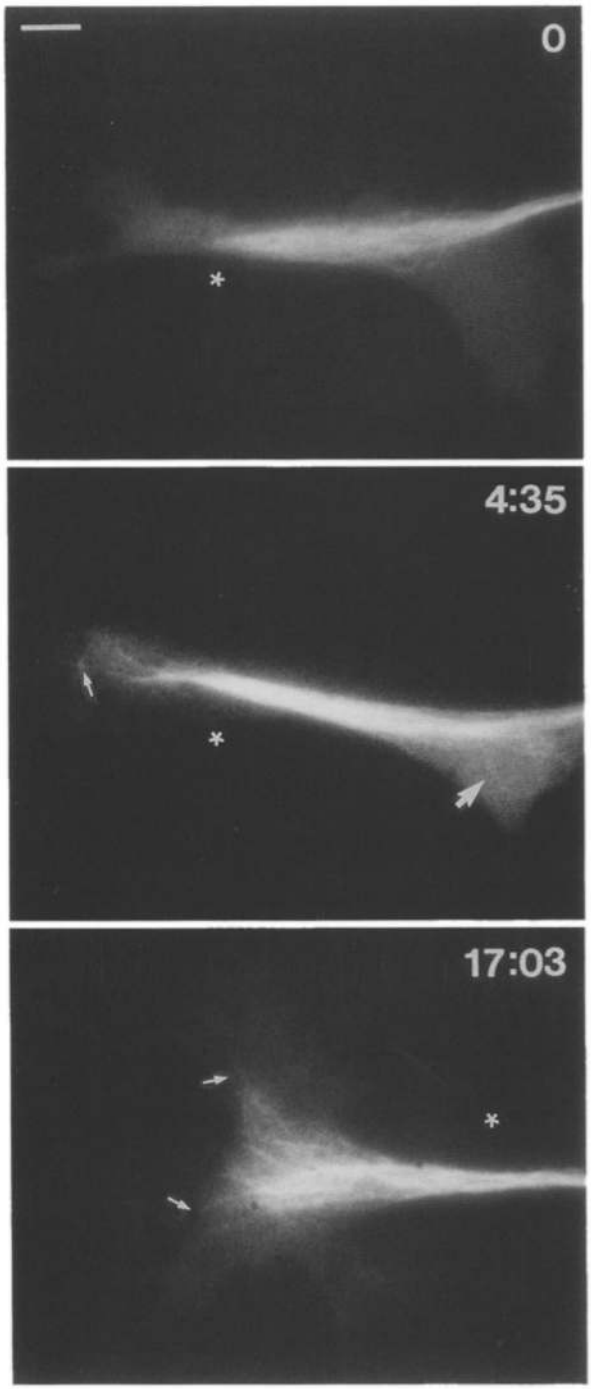

Figure 8. Recovery of the growth cone from vinblastine. At 0 min, 10 nM vinblastine has just been washed out. While a bundle remains in the growth cone, no single microtubules are evident in the distal end or the protrusion in the lower right corner. 4:35 min later, the growth cone has spread but not moved forward, and several single microtubules (*small arrow*) have merged at the distal end of the bundle, as well as several in the lower protrusion (*large arrow*). At 17:03 min, many single microtubules have repopulated the distal regions of the growth cone (*small arrows*). The growth cone at 0 and 4:35 min are in the same frame of reference. At 17:03 min, the stage was moved to keep the growth cone in the field of view. The asterisk marks a constant position in the field. The growth cone has grown ~20 μm between 4:35 and 17:03 min. Bar, 5 μm.

effects suggest that some aspect of microtubule function is intimately involved with forward movement of the growth cone. At this level of disrupting normal microtubule function, the actin-rich motile apparatus of the growth cone appears to be active, but the ability of the growth cone to continue directed movement has been compromised.

Despite the dramatic effects on growth cone extension, the effects on actin and microtubule distributions as measured statically were rather subtle. Our observations of fixed cells stained with rhodamine phalloidin showed that the distribution of actin does undergo some changes, becoming more uniform and the area of lamella decreasing somewhat. Although it has never been reported, it is formally possible that vinblastine directly affects actin distribution, and thus induces the small changes in the behavior described here. We believe that the changes in the actin distribution likely occurs via changes in microtubules because in other cell types, changes in microtubules caused by agents other than vinblastine also seem to affect the actin-based protrusive activity (6).

Vinblastine Inhibits Microtubule Dynamics in Nonneuronal Cells

Static measures of microtubule polymer levels or distribution may overlook many of its important properties connected with the action of motors or dynamic instability. In vitro experiments by Jordan et al. suggested that low doses of vinblastine inhibit dynamics but do not affect the polymer mass (24, 25, 46). We confirmed that vinblastine indeed suppressed microtubule dynamics in cells, that microtubules in cells treated with vinblastine spent much of the time in a nondynamic "paused" state, and that both growth and shrinkage rates were depressed. Although we have followed the dynamics of individual microtubules in fibroblastoid cells cultured from the neural tube, we could not determine whether the overall microtubule array is indeed more stable. In these experiments it is possible only to measure the subset of microtubules that extend sufficiently far out toward the cell periphery where the microtubule density is low. So, while it is possible that addition of vinblastine resulted in the selective depolymerization of the most dynamic microtubules, uncovering more central microtubules that are more stable and thus have different dynamic properties we believe this is unlikely to be the case. First, our findings are similar to previous results examining purified microtubules in vitro where this problem is less likely to occur (46). Second, we could sometimes observe the stabilization of dynamic microtubules. Although it is difficult to follow microtubules during perfusion of vinblastine, it was occasionally possible for us to follow previously dynamic microtubules that became stable.

After washing out vinblastine, the microtubules did not completely regain the dynamic properties that they had previous to vinblastine treatment. This may be for several reasons. First, by being stabilized with vinblastine, the polymer may have then been subject to other cellular stabilizing factors that in turn changed the properties of the microtubules, making them less dynamic. Indeed, time-dependent microtubule modifications associated with microtubule stability have been found (40, 47). Second, if the vinblastine uncovered the stable population of microtubules, they would be expected to have very different dynamic properties from dynamic microtubules, and thus may not change upon wash-

ing out vinblastine. Any new microtubules that grew from the centrosome may have taken some time to become long enough to be visualized at the cell periphery where these measurements were made.

The Effect of Vinblastine on Growth Cone Microtubules

Microtubules in growth cones during vinblastine treatment no longer underwent dynamic instability, the uncorrelated asynchronous growth and shrinkage of single microtubules. Any loops that were formed underwent slow steady, forward extension. Although we do not have direct evidence, we interpret the extension of loops to indicate translocation of polymer. These loops were persistent and resembled normal axonal growth, where microtubules could be shown by photobleaching and by other criteria to translocate forward (38, 44).

When vinblastine was washed out, straight microtubules reemerged from the distal end of the bundle and entered the lamella. The appearance of these microtubules preceded resumption of axonal growth. In contrast to the aimless wandering characteristic of vinblastine treated neurons, during recovery, neurons washout translocated directly forward and microtubule arrays would quickly become organized into single elongated bundles. We interpret these observations to mean that the presence of microtubules in the growth cone is insufficient to provide directionality for axonal growth.

Although the vinblastine may have affected microtubule dynamics in the axon as well as the growth cone, we think it most likely that changes in the dynamics of microtubules in the growth cone are the principal cause of the behavioral changes in the growth cone. First, the response of the growth cone to vinblastine is very rapid, usually less than 10 min, so it seems that the growth cone may be particularly sensitive at early time points. Indeed, local application of colcemid to cultured chick neurons showed that the growth cone is at least 100-fold more sensitive to colcemid than the axon (4). Second, previous photobleaching of fluorescent microtubule studies have shown that the most dynamic microtubules are in the growth cone. Third, it has been shown that growth cones can grow for sometime after the axon is severed from the cell body, a situation in which must dramatically affect the axonal microtubule array (22, 41). Fourth, in our fixed samples we did not notice any obvious breaks in the axon structure by fluorescence observation.

The Relationship between Microtubule Dynamics, Growth Cone Movement, and Axonal Elongation

Our observations indicate that inhibiting dynamic instability and consequently microtubule assembly stops axonal elongation. From these experiments we cannot distinguish whether the effect on axonal elongation is primarily due to inhibiting the actual dynamic properties of the microtubules or the assembly of polymer. The effects of vinblastine on neurite initiation and on long-term outgrowth have previously been interpreted as due to inhibition of assembly (3, 51). If it is continuous microtubule assembly that is required for axonal elongation these results indicate a tight coupling between microtubule assembly and neurite outgrowth. For example it is possible that the persistent movement of the growth cone is directly tied to the provision of microtubules necessary for axonal elongation. As microtubules assemble and become stable, the growth cone may be driven by some mechanism to move away from the stabilized bundle of microtubules (11, 12). Inhibiting polymerization with vinblastine would stop the supply of growing polymer. Our observation of some growth cones in which microtubules only reach the neck region during vinblastine treatment is most supportive of such a model. The subtle changes in actin distribution could also be consistent with the model. We did, however, observe a significant number of growth cones which accumulated microtubule polymer after vinblastine. This indicated that the microtubule array could still elongate under these conditions. While this may seem inconsistent with a structural role of microtubules, it is possible that while the overall array was redistributing, the inhibition of new polymer did cause a change in the compressive strength of the whole array, thus, axonal elongation could not continue.

Other studies indicate that driving microtubule polymerization, which might be expected to stimulate persistent growth cone movement and axon elongation does not drive elongation. The application of taxol to neurons, which causes microtubule polymerization inhibits normal neurite outgrowth (4, 28). Similarly, we found that when growth cones were treated with taxol, many microtubules formed but the growth cones rapidly stopped their forward progression (preliminary observations). It should be pointed out that taxol inhibits microtubule dynamics as well as promotes polymerization.

Since vinblastine inhibits the dynamic properties of microtubules as well as assembly, it is possible that dynamic microtubules themselves play a unique role in guiding the persistent movement of the growth cone, and in controlling the formation of the new axonal microtubule bundle. Our observations of vinblastine-treated neurons indicate that there is ample polymer for axonal elongation, but it never becomes organized. Furthermore, it has been found that rat superior cervical ganglia cells, when treated with low doses of vinblastine (similar to those used here) over a long period, continue to slowly extend neurites even though the microtubule polymer mass does not increase, suggesting that whatever are the residual translocation mechanisms they are sufficient to support slower, apparently more meandering outgrowth (3). In our experiments, there were a significant number of cases where microtubules accumulated in the growth cone, but did not organize into an axonal bundle and the growth cone did not advance. When vinblastine is removed and single microtubules become observable in the growth cone periphery, the stable microtubules incorporate into the axon and growth resumes.

What makes dynamic microtubules different from nondynamic ones? Perhaps only dynamic microtubules can invade a lamella through polymerization, and catalyze or act as guides for the further invasion by microtubules carrying organelles. This model would be consistent with the stages of axon formation observed for both cultured *Aplysia* and PC12 neurons. In these systems, axon formation entailed the protrusion of a lamella followed by its engorgement by organelles and the subsequent consolidation of this invaded region into an axon (2, 20). We suggest that this initial invasion of lamella by organelle-rich microtubules may need to be preceded by the polymerization of a few pioneer microtu-

bules to guide this invasion. The productive invasion of a lamella would then allow the further consolidation into an axon. Without the entry of a few initial microtubules, the stable microtubules appear to remain inert in the central region of the growth cone. In our experiments on frog neurons we always see a good correlation between the reemergence of dynamic microtubules into the growth cone periphery and the resumption of growth.

If the key event blocked by vinblastine is the invasion of the actin cortex by polymerizing microtubules (we assume that because of steric exclusion, already polymerized microtubules cannot passively enter the dense actin arrays), then it is still unclear what the consequences of this invasion are. Do the microtubules by invading the cortex create a nucleus for microtubule bundling, a picture that focuses on a failure of microtubule organization as the primary casualty of a failure to invade the actin cortex, or is the actin-rich cortex only stimulated to elongate by the microtubule invasion? At the present time, we cannot choose among these, except to note that in the absence of dynamic microtubules the growth cone still remains capable of forming lamellae. These lamellae cannot drive axonal extension. They can exert force on the growth cone and can retract, but they are incapable of forming a polarized extension that can be converted into new axon structure.

It is worth considering briefly that the dynamic growth cone microtubules' main role may not be as a structural scaffold, but as a detector of cellular conditions. During mitosis, the proper assembly of the mitotic spindle appears to be an important point of feedback control for the progression in mitosis (32). It has been suggested that cells monitor the association of microtubules with other spindle components such as kinetochores, and activate feedback control mechanisms that delay mitosis if the proper structural associations have not been made. It is possible that microtubules play an analogous role in sensing the state of the cell during neurite outgrowth. A feedback system may monitor the binding of microtubules to specific sites in the growth cone. If the proper sites are not bound, then the cell may stimulate a signal that inhibits the further consolidation of the axon. In the realm of cell signaling, many of the same molecules such as ras, the receptor tyrosine kinases, and MAP kinase, that regulate mitogenesis are important for neuronal differentiation (1, 18, 42). These and other parallels between the control of mitogenesis and control of neuronal differentiation may suggest a dual role for materials as structural and signaling components. These speculations underscore the need to look at the temporal regulation of a number of cytoskeletal and second messenger systems during neural growth and neuronal pathfinding decisions, as well as at physical interaction between microtubules and the actin cytoskeleton.

We would like to thank Doug McVey for constructing the anoxic flow chamber. We are grateful to James Sabry, David Drechsel, and Vladimir Gelfand for discussion and comments on the manuscript.

This work was supported by a grant from National Institute for General Medical Science to M. W. Krischner.

Received for publication 15 March 1994 and in revised form 27 October 1994.

References

1. Ahn, N. G., D. J. Robbins, J. W. Haycock, R. Seger, M. H. Cobb, and E. G. Krebs. 1992. Identification of an activator of the microtubule-associated kinases ERK1 and ERK2 in PC12 cells stimulated with nerve or bradykinin. *J. Neurochem.* 59:147–156.
2. Aletta, J. M., and L. A. Greene. 1988. Growth cone configuration and advance: a timelapse study using video-enhanced differential contrast microscopy. *J. Neurosci.* 8:1425–1435.
3. Baas, P. W., and F. J. Ahmad. 1993. The transport properties of axonal microtubules establish their polarity orientation. *J. Cell Biol.* 120: 1427–1437.
4. Bamburg, J. R., D. Bray, and K. Chapman. 1986. Assembly of microtubules at the tip of growing axons. *Nature (Lond.).* 321:778–790.
5. Deleted in proof.
6. Bershadsky A. D., E. A. Vaisberg, and J. M. Vasiliev. 1991. Pseudopodial activity at the active edge of migrating fibroblast is decreased after drug-induced microtubule depolymerization. *Cell Motil. Cytoskeleton.* 19: 152–158.
7. Bray, D. 1970. Surface movements during the growth of single explanted neurons. *Proc. Natl. Acad. Sci. USA.* 65:905–910.
8. Bray, D., and M. B. Bunge. 1981. Serial analysis of microtubules of cultured rat sensory neurons. *J. Neurocytol.* 10:589–605.
9. Bridgman, P. C., and M. E. Dailey. 1989. The organization of myosin and actin in rapid frozen nerve growth cones. *J. Cell Biol.* 108:95–109.
10. Bunge, M. B. 1973. Fine structure of nerve fibers and growth cones of isolated sympathetic neurons in culture. *J. Cell Biol.* 56:713–735.
11. Buxbaum, R. E., and S. R. Heidemann. 1988. A thermodynamic model for force integration and microtubule assembly during axonal elongation. *J. Theor. Biol.* 134:379–390.
12. Buxbaum, R. E., and S. R. Heidemann. 1992. An absolute rate theory model for tension control of axonal elongation. *J. Theor. Biol.* 155: 409–426.
13. Cleveland, D. W., and P. N. Hoffman. 1991. Slow axonal transport comes full circle: evidence that microtubule sliding mediates axon elongation and tubulin transport. *Cell.* 67:453–456.
14. Cyr, J. L., and S. T. Brady. 1992. Molecular motors in axonal transport. *Mol. Neurobiology.* 137–155.
15. Daniels, M. P. 1972. Colchicine inhibition of nerve fiber formation in vitro. *J. Cell Biol.* 53:164–176.
16. Daniels, M. P. 1973. Fine structural changes in neurons associated with colchicine inhibition of nerve fiber formation in vitro. *J. Cell Biol.* 58:463–470.
17. Dodd, J., and T. M. Jessell. 1988. Axon guidance and the patterning of neuronal projections in vertebrates. *Science (Wash. DC).* 242:692–699.
18. Drechsel, D. N., A. A. Hyman, M. H. Cobb, and M. W. Kirschner. 1992. Modulation of the dynamic instability of tubulin assembly by the microtubule-associated protein tau. *Mol. Biol. Cell.* 3:1141–1154.
19. Forscher, P., and S. J. Smith. 1988. Actions of cytochalasins on the organization of actin filaments and microtubules in a neuronal growth cone. *J. Cell Biol.* 107:1505–1516.
20. Goldberg, D. J., and D. W. Burmeister. 1986. Stages in axon formation: observations of growth of *Aplysia* axons in culture using video-enhanced contrast-differential interference contrast microscopy. *J. Cell Biol.* 103: 1921–1931.
21. Gordon-Weeks, P. R. 1991. Evidence for microtubule capture by filopodial actin filaments in growth cones. *Neuroreport.* 2:573–576.
22. Harris, W. A., C. E. Holt, and F. Bonhoeffer. 1987. Retinal axons with and without their somata, growing to and arborizing in the tectum of *Xenopus* embryos: a time-lapse video study of single fibres in vivo. *Development (Camb.).* 101:123–133.
23. Harrison, R. G. 1910. The outgrowth of the nerve fiber as a mode of protoplasmic movement. *J. Exp. Zool.* 17:521–544.
24. Jordan, M. A., D. Thrower, and L. Wilson. 1991. Mechanism of inhibition of cell proliferation by Vinca alkaloids. *Cancer Res.* 51:2212–2222.
25. Jordan, M. A., and L. Wilson. 1990. Kinetic analysis of tubulin exchange at microtubule ends at low vinblastine concentrations. *Biochemistry.* 29:2730–2739.
26. Keynes, R. J. 1992. Repellent cues in axon guidance. *Curr. Opin. Neurobiol.* 2:55–59.
27. Letourneau, P. C. 1981. Immunocytochemical evidence for colocalization in neurite growth cones of actin and myosin and their relationship to cell–substratum adhesions. *Dev. Biol.* 85:113–22.
28. Letourneau, P. C., and A. H. Ressler. 1984. Inhibition of neurite initiation and growth by taxol. *J. Cell Biol.* 98:1355–1362.
29. Liesi, P. 1990. Extracellular matrix and neuronal movement. *Experientia (Basel).* 46:900–907.
30. Lin, C. H., and P. Forscher. 1993. Cytoskeletal remodeling during growth cone-target interactions. *J. Cell Biol.* 121:1369–1383.
31. Lumsden, A., and J. Cohen. 1991. Axon guidance in the vertebrate central nervous system. *Curr. Opin. Genet. Dev.* 1:230–235.
32. Murray, A. W. 1992. Creative blocks: cell-cycle checkpoints and feedback controls. *Nature (Lond.).* 359:599–604.
33. Nixon, R. A. 1992. Slow axonal transport. *Curr. Opin. Cell Biol.* 4:8–14.
34. Okabe, S., and N. Hirokawa. 1989. Axonal transport. *Curr. Opin. Cell Biol.* 1:91–97.
35. Okabe, S., and N. Hirokawa 1991. Actin dynamics in growth cones. *J. Neurosci.* 11:1918–1929.

36. Palka, J., K. E. Whitlock, and M. A. Murray. 1992. Guidepost cells. *Curr. Opin. Neurobiol.* 2:48–54.
37. Peters, A., S. L. Palay, and H. Webster. 1991. The fine structure of the nervous system: neurons and their supporting cells. W. B. Saunders, Philadelphia.
38. Reinsch, S. S., T. J. Mitchison, and M. W. Kirschner. 1991. Microtubule polymer assembly and transport during axonal elongation. *J. Cell Biol.* 115:1364–1380.
39. Sabry, J. H., T. P. O'Connor, L. Evans, A. Toroian-Raymond, M. W. Kirschner, and D. Bentley. 1991. Microtubule behavior during guidance of pioneer neurons growth cones in situ. *J. Cell Biol.* 115:1381–1395.
40. Schulze, E., D. J. Asai, J. C. Bulinski, and M. Kirschner. 1987. Posttranslational modification and microtubule stability. *J. Cell Biol.* 105: 2167–2177.
41. Shaw, G., and D. Bray. 1977. Movement and extension of isolated growth cones. *Exp. Cell Res.* 104:55–62.
42. Shibuya, E. K., T. G. Boulton, M. H. Cobb, and J. V. Ruderman. 1992. Activation of p42 MAP kinase and the release of oocytes from arrest. *EMBO (Eur. Mol. Biol. Organ.) J.* 11:3963–75.
43. Symons, M., and T. J. Mitchison. 1991. Control of actin polymerization in live and permeabilized fibroblasts. *J. Cell Biol.* 114:503–513.
44. Tanaka, E., and M. Kirschner. 1991. Microtubule behavior in the growth cones of living neurons during axon elongation. *J. Cell Biol.* 115: 345–363.
45. Tessier-Lavigne, M. 1992. Axon guidance by molecular gradients. *Curr. Opin. Neurobiol.* 2:60–65.
46. Toso, R. J., M. A. Jordan, K. W. Farrell, B. Matsumoto, and L. Wilson. 1993. Kinetic stabilization of microtubule dynamic instability in vitro by vinblastine. *Biochemistry.* 32:1285–1293.
47. Webster, D. R., G. G. Gundersen, J. C. Bulinski, and G. G. Borisy. 1987. Differential turnover of tyrosinated and detyrosinated microtubules. *Proc. Natl. Acad. Sci. USA.* 84:9040–9044.
48. Wessells, N. K., and R. P. Nuttall. 1978. Normal branching, induced branching, and steering of cultured parasympathetic motor neurons. *Exp. Cell Res.* 115:111–122.
49. Yamada, K. M., B. S. Spooner, and N. K. Wessells. 1970. Axon growth: role of microfilaments and microtubules. *Proc. Natl. Acad. Sci. USA.* 66:1206–1212.
50. Yamada, K. M., B. S. Spooner, and N. K. Wessells. 1971. Ultrastructure and function of growth cones and axons of cultured nerve cells. *J. Cell Biol.* 49:614–635.
51. Zheng, J., R. E. Buxbaum, and S. R. Heidemann. 1993. Investigation of microtubule assembly and organization accompanying tension-induced neurite initiation. *J. Cell Sci.* 104:1239–1250.